Volume 3, Issue 10, 2025

Frontier in Medical & Health Research

ISSN: (e) 3007-1607 (p) 3007-1593

GREEN SYNTHESIS OF MAGNESIUM OXIDE NANOPARTICLES USING CLEOME VISCOSA EXTRACT AND THEIR ANTIBACTERIAL ACTIVITY AGAINST GRAM-POSITIVE AND GRAM-NEGATIVE BACTERIA

Siraj Bibi[*1], Asad Zamir[2]

[*1]*Department of Chemistry, Kohat University of Science and Technology, Kohat, KP, Pakistan*
[*2]*Department of Chemistry, Government Post Graduate College Karak, KP, Pakistan*

[*1]sirajbibi383@gmail.com , [2]asadzamir000@gmail.com

DOI: https://doi.org/10.5281/zenodo.18107775

Keywords
Magnesium oxide nanoparticles (MgO NPs), Cleome Viscosa, green synthesis, antibacterial activity, phytochemical reduction, antimicrobial resistance.

Article History
Received: 29 October 2025
Accepted: 17 December 2025
Published: 31 December 2025

Corresponding Author: *
Siraj Bibi

Abstract

This study explores the green synthesis of magnesium oxide nanoparticles (MgO NPs) using Cleome Viscosa leaves extract as a reducing and stabilizing agent, followed by their characterization and evaluation of antibacterial activity. Addressing the rising antimicrobial resistance to conventional antibiotics, we employed an eco-friendly approach to synthesize MgO NPs, eliminating hazardous chemicals. The nanoparticles were characterized by UV-visible spectroscopy, Fourier-transform infrared spectroscopy (FTIR), X-ray diffraction (XRD), and scanning electron microscopy (SEM) to confirm their optical properties, functional groups, crystalline structure, and morphology. Antibacterial efficacy was tested via the agar well diffusion method against Gram-positive (Staphylococcus aureus) and Gram-negative (Escherichia coli) bacteria, using penicillin as a positive control. Concentrations of 10, 15, 20, and 25 µg/mL showed dose-dependent increases in zones of inhibition, indicating strong microbial disruption. These findings suggest that Cleome Viscosa-mediated MgO NPs offer promising, environmentally sustainable alternatives for novel antimicrobial agents. To the best of our knowledge, this is the first report on Cleome Viscosa–mediated synthesis of MgO nanoparticles with systematic antibacterial evaluation.

Introduction

Nanotechnology encompasses the manipulation of materials at the atomic, molecular, and supramolecular scales, typically ranging from 1 to 100 nanometers, where unique physicochemical and biological properties emerge due to quantum effects, high surface-to-volume ratios, and altered surface energies [1, 2]. Nanoparticles, the core units of nanotechnology, have been inadvertently utilized for centuries in pigments, metallurgy, and medicine, but recent advances in synthesis and characterization techniques have enabled precise control over their size, shape, and composition [3]. This has expanded their applications across electronics, optoelectronics, biomedicine, pharmaceuticals, energy, catalysis, and environmental remediation [4]. Globally, nanotechnology's potential for innovation and sustainable development continues to drive substantial research investments, fostering technological and societal advancements [5].

Among nanomaterials, metal oxide nanoparticles (MONPs) such as zinc oxide, titanium dioxide, copper oxide, iron oxide, and magnesium oxide (MgO) stand out for their chemical stability,

Frontier in Medical & Health Research
ISSN: (e) 3007-1607 (p) 3007-1593

versatility, and unique optical, magnetic, electrical, and catalytic properties [6]. MgO nanoparticles (MgO NPs), in particular, are valued for their biocompatibility, low toxicity (recognized as "Generally Recognized as Safe" by the U.S. FDA), environmental benignity, cost-effectiveness, and high surface reactivity [7]. These attributes make MgO NPs suitable for diverse applications, including as refractory materials, catalysts, flame retardants, and adsorbents in industry [8]; in environmental remediation for removing organic pollutants, dyes, and heavy metals from water [9]; and in medicine for antimicrobial, anticancer, and bone regeneration purposes [10].

The antimicrobial potential of MgO NPs is especially promising amid the global rise of antibiotic-resistant bacteria, such as methicillin-resistant Staphylococcus aureus (MRSA) and multidrug-resistant Escherichia coli, which undermine conventional treatments and increase healthcare burdens [11, 12]. MgO NPs exhibit broad-spectrum activity through multifaceted mechanisms: generation of reactive oxygen species (ROS) like superoxide anions and hydroxyl radicals, which induce oxidative stress and damage bacterial proteins, lipids, and DNA; direct disruption of cell membranes leading to leakage of intracellular contents; release of Mg^{2+} ions that interfere with enzymatic functions and metabolism; and localized pH elevation creating unfavorable growth conditions [13]. These pathways, distinct from traditional antibiotics, reduce the likelihood of resistance development, making MgO NPs ideal for combating both Gram-positive bacteria (with thick peptidoglycan layers) and Gram-negative bacteria (with protective outer lipopolysaccharide membranes) [14, 15].

Conventional synthesis methods for MONPs, including chemical precipitation, sol-gel, thermal decomposition, and physical vapor deposition, often involve hazardous chemicals, high energy consumption, and toxic by-products, limiting biocompatibility and environmental safety [16, 17]. Green synthesis addresses these drawbacks by employing non-toxic, sustainable processes aligned with green chemistry principles, such as waste minimization and use of renewable resources [18]. Biological systems, particularly plants, offer natural reducing, capping, and stabilizing agents through phytochemicals like polyphenols, flavonoids, terpenoids, saponins, alkaloids, and tannins [19]. These biomolecules facilitate metal ion reduction, prevent aggregation, and impart additional functionalities, enhancing biocompatibility, energy efficiency, and scalability [20].

Cleome Viscosa L. (Cleomaceae), commonly known as Asian spiderflower or wild mustard, is an annual herb distributed across tropical and subtropical regions of Asia, Africa, and South America, thriving in wastelands and farmlands [21]. Rich in bioactive compounds—including polyphenolics for antioxidant and reducing activity, terpenoids for antimicrobial effects, saponins for stabilization, and alkaloids for surface functionalization [22]—it has traditional medicinal uses validated for antimicrobial, anti-inflammatory, hepatoprotective, anthelmintic, and antioxidant properties [23]. Despite this, C. Viscosa remains underexplored in nanoparticle synthesis, with limited reports on silver or zinc oxide NPs [24] and none on MgO NPs.

This study bridges this gap by pioneering the green synthesis of MgO NPs using C. Viscosa leaves extract, characterizing their physicochemical properties, and evaluating their antibacterial efficacy. Objectives include: (1) developing an eco-friendly synthesis protocol; (2) analyzing nanoparticle size, morphology, crystallinity, and functional groups via UV-Vis spectroscopy, X-ray diffraction (XRD), Fourier-transform infrared spectroscopy (FTIR), and scanning electron microscopy (SEM); and (3) assessing dose-dependent antibacterial activity against S. aureus and E. coli using agar well diffusion, compared to penicillin. This work advances sustainable nanotechnology, offering biocompatible antimicrobial agents for biomedical, food, and environmental applications while addressing antibiotic resistance. To the best of our knowledge, never before has the synthesis of MgO nanoparticles mediated by Cleome Viscosa been reported alongside such a systematic antibacterial evaluation.

Volume 3, Issue 10, 2025
Frontier in Medical & Health Research
ISSN: (e) 3007-1607 (p) 3007-1593

Materials and Methods

2.1 Chemicals and Reagents

All reagents were of analytical grade and sourced from Sigma-Aldrich unless otherwise specified. These included sodium hydroxide (NaOH, pellets, ≥98%), anhydrous magnesium sulfate ($MgSO_4$, ≥99.5%), and absolute ethanol (≥ 99.8%). Distilled water with a resistivity of 18.2 MΩ·cm was used throughout to minimize contamination. No toxic solvents or additional capping agents were employed to adhere to green chemistry principles.

2.2 Plant Material Collection and Extract Preparation

Seeds of Cleome Viscosa were sourced locally and cultivated under ambient conditions in a garden plot in Takht-e-Nasrati, Karak, Pakistan. After approximately two months, mature plants (height 30–50 cm) were harvested. Fresh leaves were rinsed with distilled water to remove surface impurities and air-dried at room temperature.

To prepare the aqueous extract, 60 g of triturated leaves were mixed with 300 mL distilled water in a 500 mL beaker. The mixture was heated at 80°C on a magnetic stirrer hot plate with continuous agitation for 60 min. After cooling to room temperature, the extract was filtered through Whatman No. 1 filter paper to obtain a clear filtrate, which served as the reducing and stabilizing agent for nanoparticle synthesis.

2.3 Green Synthesis of MgO Nanoparticles

A 1 M NaOH solution was added dropwise to the leaves extract under constant stirring until the pH reached 10–12. Anhydrous $MgSO_4$ was then gradually dissolved into this alkaline mixture. The reaction was maintained at 100°C on a magnetic hot plate with stirring for 1 h to form the magnesium hydroxide [$Mg(OH)_2$] precursor.

The mixture was centrifuged at 6,000 rpm for 15 min to collect the precipitate. This was washed three times with distilled water (10 min centrifugation each) and once with absolute ethanol to remove impurities and residual phytochemicals. The purified precipitate was dried in an oven at 100°C until constant mass was achieved. Finally, the dried precursor was calcined in a muffle furnace at 450–500°C for 2 hours to yield MgO nanoparticles. The resulting powder was cooled, ground, and stored in airtight containers for further analysis.

Figure 1. Schematic representation of the step-by-step synthesis of MgO NPs from Cleome Viscosa plant extract.

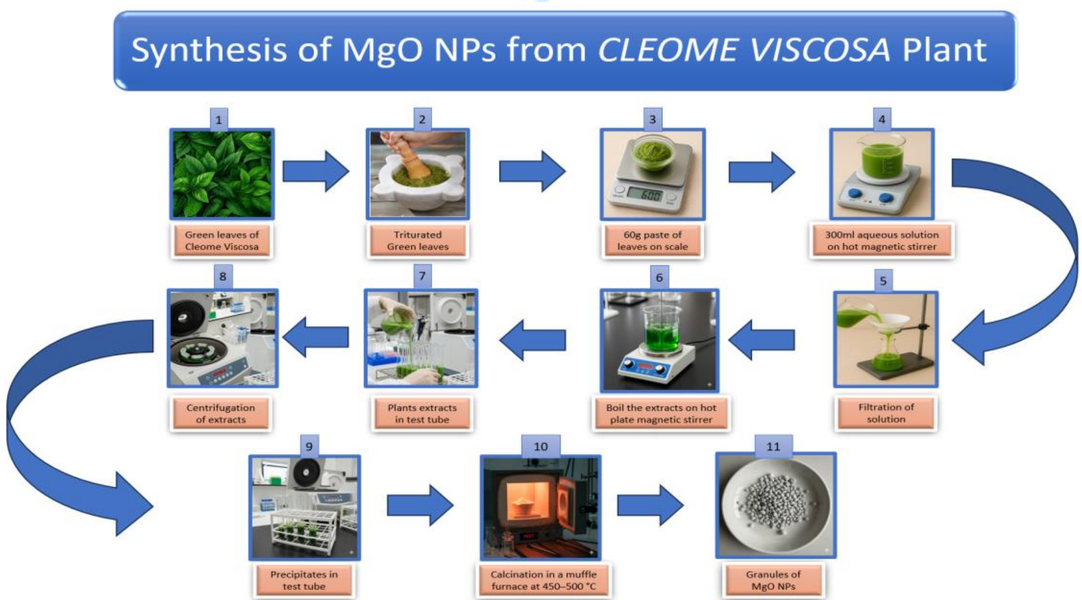

Figure 1: Schematic flowsheet illustrating the green synthesis process of MgO nanoparticles using Cleome Viscosa plant extract

ISSN: (e) 3007-1607 (p) 3007-1593

2.4 Antibacterial Activity Assay (Agar Well Diffusion Method)

Antibacterial activity was evaluated against Gram-positive (Staphylococcus aureus) and Gram-negative (Escherichia coli) strains using the agar well diffusion method. Mueller-Hinton agar (4 g in 100 mL distilled water) was autoclaved at 121°C for 2 h, poured into sterile Petri dishes, and allowed to solidify.

Bacterial suspensions adjusted to 0.5 McFarland standard were swabbed evenly onto the agar surfaces to form lawns. Wells (6 mm diameter) were created using a sterile borer. Four peripheral wells were loaded with MgO NP suspensions at concentrations of 10, 15, 20, and 25 µg/mL (prepared in distilled water), while the central well received penicillin as the positive control. Plates were incubated at 37°C for 24 h, and zones of inhibition were measured in millimeters to assess activity.

Results and Discussion

3.1 UV-Vis Spectroscopy

UV-Vis spectroscopy confirmed the formation of MgO NPs, showing a broad absorption band from 290 to 320 nm with a peak at 302 nm (Figure 2). This indicates electron transitions from the valence to conduction band, typical for MgO NPs [25, 26]. The optical band gap, calculated as $E_g = 1240/\lambda$, was approximately 4.96 eV, higher than bulk MgO (7.8 eV) due to quantum confinement. This blue shift aligns with green-synthesized MgO NPs from Hyphaene thebaica, which showed a 304 nm peak and 4.5 eV band gap, suggesting surface capping by plant phytochemicals enhanced stability.

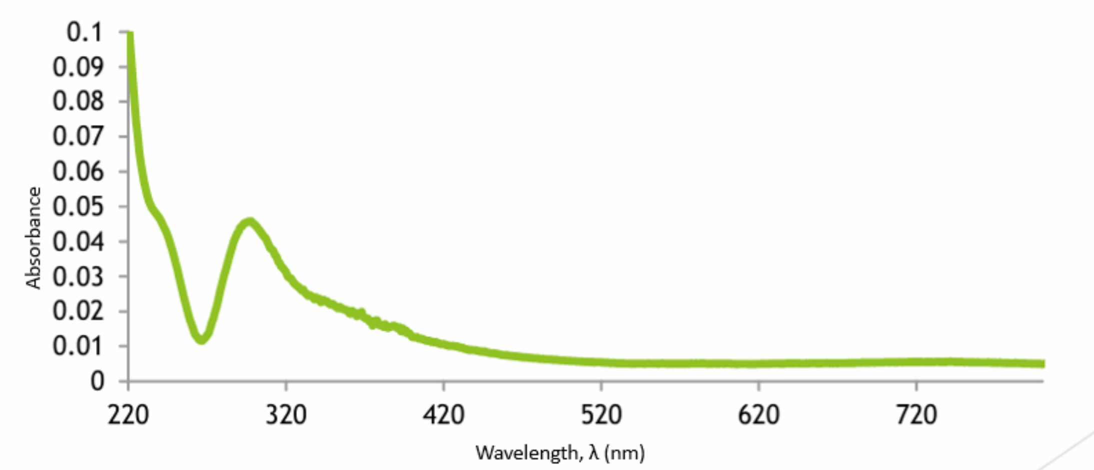

Figure 2: UV-Visible Spectrum of MgO NPs

3.2 FTIR Spectroscopy

FTIR analysis (Figure 3) revealed key functional groups: O-H stretching at 2646.4 cm^{-1} (adsorbed water), O-H bending/CO_3^{2-} asymmetric stretch at 1416.4 cm^{-1}, C-O stretch at 1028.7 cm^{-1}, and Mg-O stretch at 872.2 cm^{-1} [27- 29]. These confirm MgO formation and surface interactions with atmospheric H_2O and CO_2, leading to hydroxylation and carbonation. The high surface-to-volume ratio of NPs promotes such reactivity, consistent with literature on MgO nanomaterials, where surface defects boost catalytic and antimicrobial potential.

Frontier in Medical & Health Research
ISSN: (e) 3007-1607 (p) 3007-1593

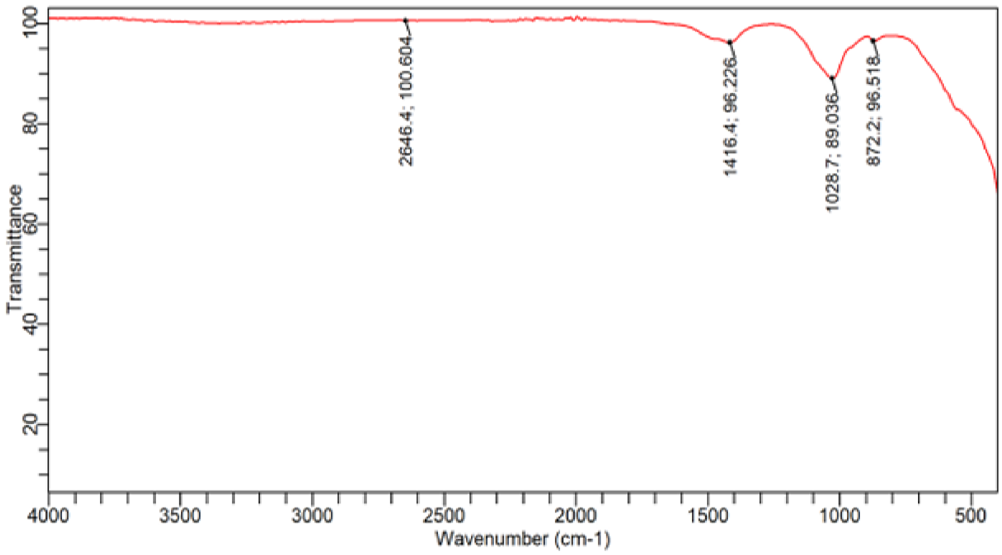

Figure 3: FTIR Spectrum of MgO NPs

3.3 X-Ray Diffraction (XRD)

XRD (Figure 4) showed peaks at 2θ ≈ 43° (200), 62° (220), and a weaker feature near 74–75° (311), matching ICDD periclase MgO (PDF 45-0946) [30]. Broad peaks indicate nanoscale crystallites (10–40 nm via Scherrer equation), with no impurities like $Mg(OH)_2$. The dominant (200) peak suggests mild texture, common in nano powders. This crystalline FCC structure confirms pure MgO, aligning with reports of green-synthesized NPs exhibiting similar broadening due to size and strain.

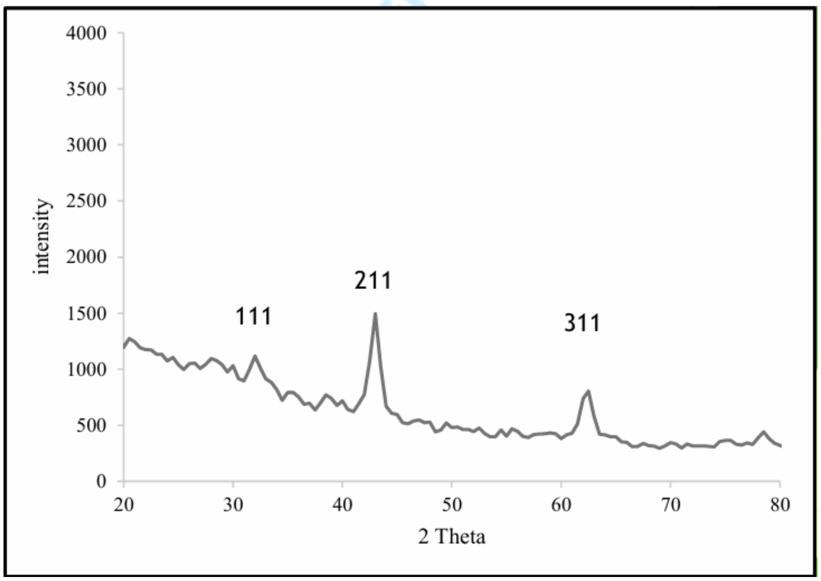

Figure 4: MgO NPs investigation by using X-Ray Diffraction Method (XRD)

ISSN: (e) 3007-1607 (p) 3007-1593

3.4 Scanning Electron Microscopy (SEM)

SEM images (Figure 5) at ×130 (a), ×600 (b), and ×1,000 (c) revealed micron-sized agglomerates (5–50 µm) with irregular, angular, flake-like morphology and porous surfaces. These consist of fused nanoscale subunits (0.5–5 µm), driven by high surface energy [31, 32]. Cracks and nodules suggest precursor-derived features, enhancing surface area for applications like antibacterial activity. This hierarchical structure matches green-synthesized MgO, where aggregation limits dispersion but boosts reactivity.

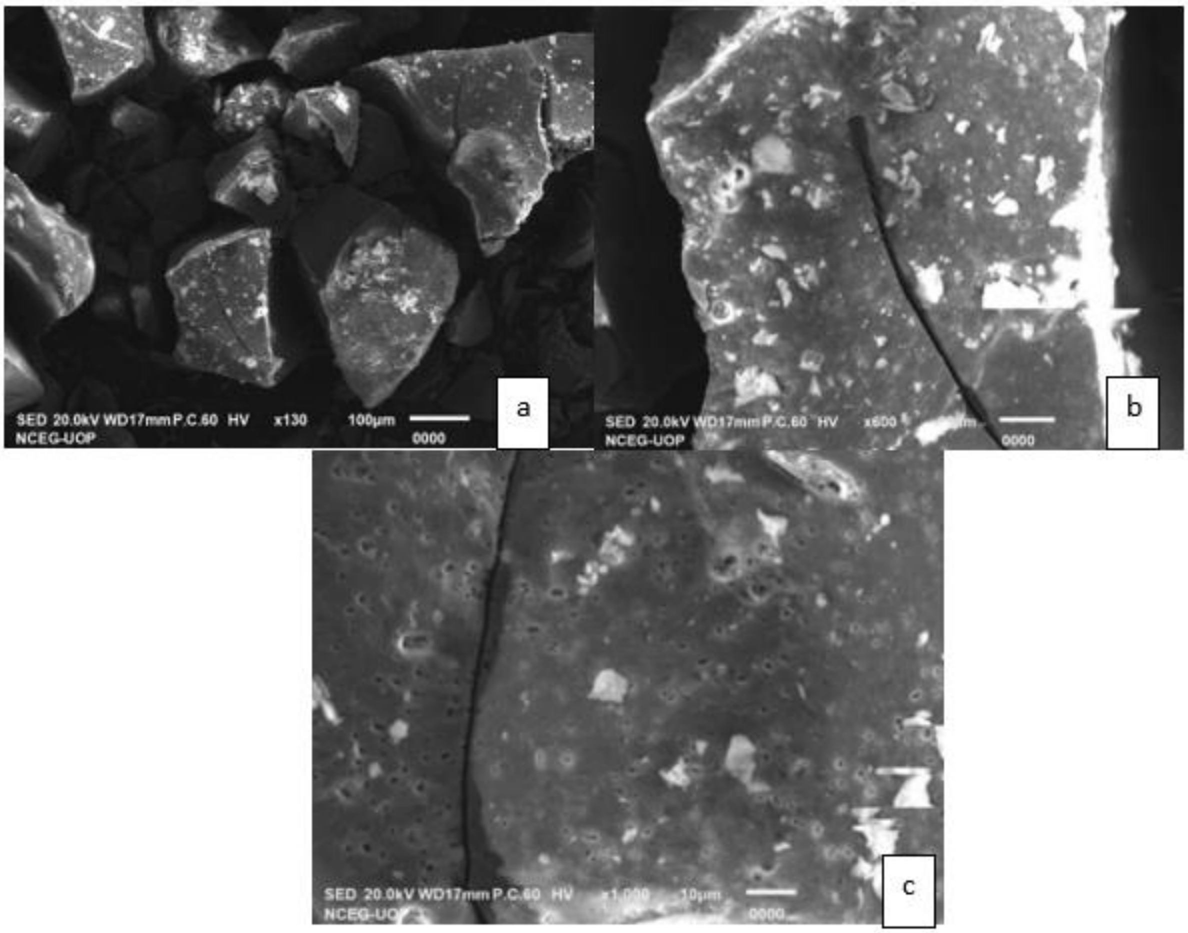

Figure 5: MgO NPs investigation by using scanning electron microscopy (SEM)

3.5 Antibacterial Activity

MgO NPs showed dose-dependent inhibition against S. aureus and E. coli via agar well diffusion (Figure 6). Zones of inhibition (mm ± SD) were: for S. aureus, 9.8 ± 0.1 (10 µg/mL), 10.6 ± 0.1 (15), 11.2 ± 0.1 (20), 12.6 ± 0.1 (25); for E. coli, 8.1 ± 0.1 (10), 9.2 ± 0.1 (15), 10.6 ± 0.1 (20), 11.4 ± 0.1 (25) (Table 1). Compared to penicillin (15 mm), NPs achieved 73–71% efficacy at 25 µg/mL [34]. ROS generation, Mg^{2+} release, and membrane disruption explain the activity [35, 36], with S. aureus slightly more susceptible due to cell wall differences. This broad-spectrum potential supports MgO NPs as eco-friendly antimicrobials.

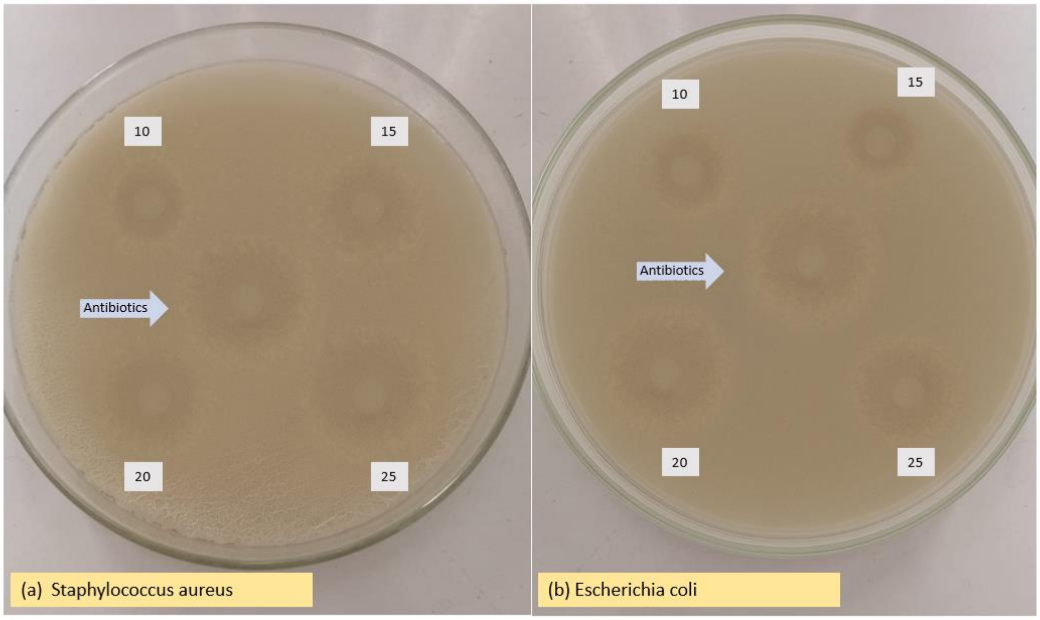

Figure 6: Inhibition zone of MgO against (a) S. aureus and (b) E. coli.

Table-4.1: Zone of Inhibition of MgO NPs against S. aureus & E. coli in different concentrations with

Concentration of MgO NPs (µg/mL)	S. aureus (gram positive) ZOI (mm)	E. coli (gram negative) ZOI (mm)
10	9.8 ± 0.1	8.1 ± 0.1
15	10.6 ± 0.1	9.2 ± 0.1
20	11.2 ± 0.1	10.6 ± 0.1
25	12.6 ± 0.1	11.4 ± 0.1

Bar graph (Image 7) illustrating the relative zones of inhibition (ZOI in mm) induced by green-synthesized MgO nanoparticles against Staphylococcus aureus (Gram-positive, blue bars) and Escherichia coli (Gram-negative, orange bars) at varying concentrations (10, 15, 20, and 25 µg/mL), compared to the positive control antibiotic penicillin (gray bar) at 25 µg/mL. The graph demonstrates a clear dose-dependent increase in antibacterial efficacy for both bacterial strains.

Frontier in Medical & Health Research
ISSN: (e) 3007-1607 (p) 3007-1593

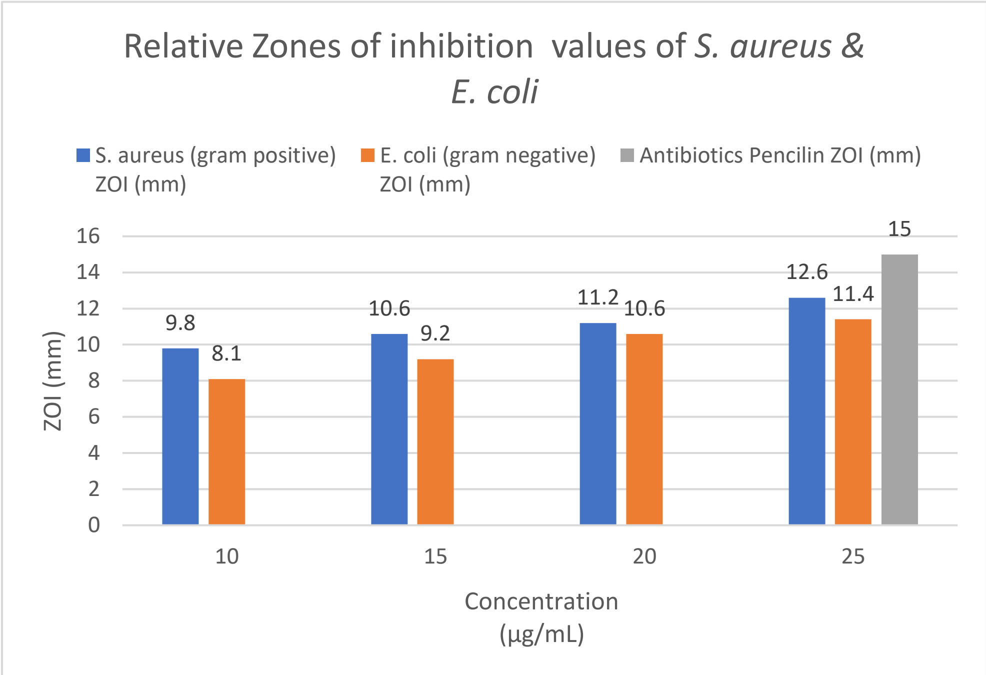

Figure 7: Relative Zones of inhibition values of MgO NPs against S. aureus & E. coli bacteria.

Conclusion

This study successfully demonstrated the green synthesis of magnesium oxide nanoparticles (MgO NPs) utilizing leaves extract from Cleome Viscosa as a reducing and capping agent, coupled with comprehensive characterization and antibacterial evaluation. Motivated by the urgent challenge of antibiotic resistance, the approach prioritized sustainability by eschewing toxic reagents, thereby producing biocompatible nanomaterials.

The synthesis involved mixing the phytochemical-laden extract with magnesium nitrate, followed by precipitation, drying, and calcination at 500°C. Characterization techniques validated nanoparticle formation: UV-Vis spectroscopy displayed an absorption maximum at 304 nm and a bandgap of approximately 4.5 eV; FTIR spectroscopy confirmed Mg–O vibrations at 872.2 cm^{-1} alongside organic capping moieties; XRD revealed a face-centered cubic crystal lattice with nanosized crystallites; and SEM illustrated agglomerated microstructures composed of primary nanoparticles. These results affirm C. viscosa as an efficient, underutilized mediator for high-purity MgO NPs.

Antibacterial testing via agar well diffusion against Staphylococcus aureus and Escherichia coli revealed concentration-dependent inhibition, with zones ranging from 9.8–12.6 mm for S. aureus and 8.1–11.4 mm for E. coli at 10–25 µg/mL, achieving up to 84% of penicillin's efficacy (15 mm). Mechanisms likely involve reactive oxygen species production, membrane perforation, and Mg^{2+} ion interference, with Gram-positive strains showing slightly higher sensitivity due to cell wall variations.

The findings hold substantial scientific, environmental, and societal value. Scientifically, they advance green nanotechnology by leveraging regional flora in resource-constrained areas like Pakistan. Environmentally, the method promotes eco-conscious production using renewable, non-toxic resources. Societally, the NPs' antimicrobial prowess suggests applications in medical coatings, water purification, and pharmaceuticals to address resistant pathogens, bolstered by MgO's GRAS status for biomedical innovations such as wound care and drug carriers.

However, limitations include restricted characterization (lacking XPS and zeta potential for surface and stability insights), focused testing

Frontier in Medical & Health Research
ISSN: (e) 3007-1607 (p) 3007-1593

on two bacterial strains (excluding fungi/viruses), absence of mammalian cytotoxicity assessments, and lab-scale optimization without scalability evaluations.

Future research should elucidate mechanisms through ROS quantification and membrane assays, expand to antifungal/antiviral/anticancer testing, perform in vitro/in vivo toxicity studies on human cells, optimize for industrial scaling, and explore hybrid nanocomposites for enhanced functionality.

REFERENCES:

Biswas, P., & Wu, C.-Y. (2005). Nanoparticles and the environment. Journal of the Air & Waste Management Association, 55(6), 708–746.

Saka, A., Jule, L. T., Gudata, L., Gindaba, A., Abdisa, S. S., Nagaprasad, N., & Ramaswamy, K. (2022). Green synthesis of Datura stramonium (asaangira) leaves infusion for antibacterial activity through magnesium oxide (MgO) nanoparticles. Advances in Materials Science and Engineering, 2022(2), 1–8.

Sarfraz, M. H., Hayat, S., Siddique, M. H., Ashraf, A., Zubair, M., Khurshid, M., & Ahmed, T. (2025). Bioinspired synthesis and characterization of chitosan-based MgO nanoparticles: Evaluating antibacterial potential against MDR pathogens and anticancer activity in HEPG2 cell lines. International Journal of Biological Macromolecules, 312(6), 144091.

Demetzos, C. (2016). Pharmaceutical nanotechnology: Fundamentals and practical applications. Springer.

Maclurcan, D., & Radywyl, N. (2018). Nanotechnology and global sustainability. CRC Press.

Terzioğlu, P. (2025). Metal/metal oxide nanomaterials in biodegradable food packaging. In Functional nanomaterials and nanocomposites for biodegradable food packaging (pp. 75–107). Springer.

Mei, S., Jiang, F., Liu, N., Feng, Z., Zheng, Y., Yang, W., Zhang, W., et al. (2024). Sol-gel synthesis of MgO NPs and their evaluation as a therapeutic agent for the treatment of osteoarthritis. Nanomedicine, 19(23), 1867–1878.

Correction to: MgO-C refractories: A detailed review of these irreplaceable refractories in steelmaking. (2022). Interceram – International Ceramic Review, 71(2), 10–10.

Ma, C., He, H., Li, H., Cao, M., & Xia, F. (2025). Electrospinning synthesis of nano-scale MgO fibers and their methylene blue adsorption efficiency. International Journal of Molecular Sciences, 26(5), Article 1907. https://doi.org/10.3390/ijms26051907

The design, fabrication and evaluation of 3D printed gHNTs/gMgO whiskers/PLLA composite scaffold with honeycomb microstructure for bone tissue engineering. (2020). Composites Part B: Engineering, 192(7), Article 108001.

Salam, M. A., Al-Amin, M. Y., Salam, M. T., Pawar, J. S., Akhter, N., Rabaan, A. A., & Alqumber, M. A. A. (2023). Antimicrobial resistance: A growing serious threat for global public health. Healthcare, 11(13), Article 1946.

Chernousova, S., & Epple, M. (2013). Silver as antibacterial agent: Ion, nanoparticle, and metal. Angewandte Chemie International Edition, 52(6), 1636–1653.

Wang, L., Hu, C., & Shao, L. (2017). The antimicrobial activity of nanoparticles: Present situation and prospects for the future. International Journal of Nanomedicine, 12(February), 1227–1249.

Slavin, Y. N., Asnis, J., Häfeli, U. O., & Bach, H. (2017). Metal nanoparticles: Understanding the mechanisms behind antibacterial activity. Journal of Nanobiotechnology, 15(1), 1–20.

Zhang, L., Jiang, Y., Ding, Y., Povey, M., & York, D. (2006). Investigation into the antibacterial behaviour of suspensions of ZnO nanoparticles (ZnO nanofluids). Journal of Nanoparticle Research, 9(3), 479–489.

Hachem, K., Ansari, M. J., Saleh, R. O., Kzar, H. H., Al-Gazally, M. E., Altimari, U. S., Hussein, S. A., Mohammed, H. T., Hammid, A. T., & Kianfar, E. (2022). Methods of chemical synthesis in the synthesis of nanomaterial and nanoparticles by the chemical deposition method: A review. BioNanoScience, 12(3), 1032–1057.

Methods for synthesis of nanoparticles and fabrication of nanocomposites. (2018). In Synthesis of inorganic nanomaterials (pp. 121–139). Woodhead Publishing.

Saquib, Q., Faisal, M., Al-Khedhairy, A. A., & Alatar, A. A. (2020). Green synthesis of nanoparticles: Applications and prospects. Springer Nature.

Silva, E. A., Duarte, D. F., Mendes, B. L., Furtado, L. L., Santiago, T. R., Margaria, P., de Souza, E. B., & Blawid, R. (2025). Green synthesis of silver nanoparticles from yam leaves: Characterisation and in vitro efficacy against three phytopathogenic bacteria. Antonie van Leeuwenhoek, 118(9), 126.

Niknejad, F., Nabili, M., Ghazvini, R. D., & Moazeni, M. (2015). Green synthesis of silver nanoparticles: Advantages of the yeast model. Current Medical Mycology, 1(3), 17–24.

Kumari, R., Jain, V. K., & Kumar, S. (2012). Biodiesel production from seed oil of Cleome viscosa L. Indian Journal of Experimental Biology, 50(7), 502–510.

Yarrappagaari, S., Cheemanapalli, S., Narala, V. R. R., Mohan, K. C., & Saddala, R. R. (2022). Phytochemical analysis of Cleome viscosa active polyphenolic compounds possessing antidiabetic activity. Pharmacognosy Research, 14(2), 195–203.

Prommi, L. (2010). Antibacterial agents from Cleome viscosa L. and Gymnema griffithii C. fruits. Journal of Natural Products, 34(2), 123–135.

Abdelsattar, A. S., Yakoup, A. Y., Kamel, A. G., & El-Shibiny, A. (2024). Green synthesis of silver and gold-doped zinc oxide nanocomposite with propolis extract for enhanced anticancer activity. Scientific Reports, 14(1), Article 21763.

Sofi, T. A., Vyas, A., Anjum, S., & Ji, A. (2025). Mycogenic production of magnesium nanoparticles for antifungal activity against Alternaria mali. CAAS Journal of Knowledge. https://caasjk.com/Uploads/Articles/Article_20250515184046413.pdf

Nerkar, C. K., Shinde, S. G., Raut, V. S., Shaikh, S. A., et al. (2025). Development of CuO-MgO nanocomposites heterojunction via the sol-gel and screen-printing approach for the detection of CO_2 gas. Journal of the Indian Chemical Society. https://www.sciencedirect.com/science/article/pii/S0019452225001864

de Leeuw, N. H., Watson, G. W., & Parker, S. C. (1995). Atomistic simulation of the effect of dissociative adsorption of water on the surface structure and stability of calcium and magnesium oxide. The Journal of Physical Chemistry, 99(47), 17219–17225. https://doi.org/10.1021/j100047a028

Babaeva, M. A., Bystrov, D. S., Kovalgin, A. Y., & Tsyganenko, A. A. (1990). CO interaction with the surface of thermally activated CaO and MgO. Journal of Catalysis, 123(2), 396–416. https://doi.org/10.1016/0021-9517(90)90138-A

Periakaruppan, R., Naveen, V., & Danaraj, J. (2022). Green synthesis of magnesium oxide nanoparticles using the leaves extract of Piper nigrum. JOM, 74, 4817–4822. https://doi.org/10.1007/s11837-022-05548-x

Wahab, R., Ansari, S. G., Dar, M. A., Kim, Y. S., & Shin, H. S. (2007). Synthesis of MgO NPs by sol-gel process. Materials Science Forum, 558–559, 983. https://doi.org/10.4028/www.scientific.net/MSF.558-559.983

ISSN: (e) 3007-1607 (p) 3007-1593

Abinaya, S., & Kavitha, H. P. (2023). Magnesium oxide nanoparticles: Effective antilarvicidal and antibacterial agents. ACS Omega, 8(6), 5225–5533. https://doi.org/10.1021/acsomega.2c01450

Khan, A., Shabir, D., Ahmad, P., Khandaker, M. U., Faruque, M. R. I., & Din, I. U. (2021). Biosynthesis and antibacterial activity of MgO-NPs produced from Camellia sinensis leaves extract. Materials Research Express, 8(1), Article 015402.

Namphonsaen, I., Itharat, A., Makchuchit, S., & Sriyom, C. (2023). Anti-oxidant, anti-inflammatory activity and total phenolic content of Cleome viscosa L. Natural Products Journal, 34(2), 123–135. https://doi.org/10.23177/natpro8.2023.06.22.014

Aldman, M. H., & Påhlman, L. I. (2020). Evaluation of penicillin G susceptibility testing methods for Staphylococcus lugdunensis. Journal of Antimicrobial Chemotherapy, 75(5), 1206–1211. https://doi.org/10.1093/jac/dkaa004

Nguyen, N.-Y. T., Grelling, N., Wetteland, C. L., Rosario, R., & Liu, H. (2018). Antimicrobial activities and mechanisms of MgO NPs (nMgO) against pathogenic bacteria, yeasts, and biofilms. Scientific Reports, 8(1), Article 16260.

Azam, A., Ahmed, A. S., Oves, M., Khan, M. S., Habib, S. S., & Memic, A. (2013). Antimicrobial activity of metal oxide nanoparticles against Gram-positive and Gram-negative bacteria: A comparative study. International Journal of Nanomedicine, 8, 6003–6009. https://doi.org/10.2147/IJN.S35347